Simulation And Design of Rocket Propulsion Nozzles

Jovanny Shek

Abstract

Nozzle geometry is one of the most important design decisions in rocket propulsion, yet it is also one of the most constrained. Traditional design methods usually determine the nozzle shape based on a single operating condition, accepting potential losses across the rest of the flight envelope as a necessary compromise. This project challenges this approach by treating the nozzle contour as an optimizable variable instead of a fixed one.

A simulation is developed based on one-dimensional isentropic flow theory, with a cosine divergence correction applied to account for off-axis exhaust momentum. The nozzle geometry is parameterized as a discrete radius profile of ten points along a fixed axial length, giving the optimizer direct control over the full contour shape rather than a small number of scalar parameters. Performance is evaluated across a range of ambient pressures to study how the optimal design changes with altitude.

The simulation was tested against 14 real engine configurations, including the NASA RS-25, SpaceX Merlin 1D in both sea-level and vacuum variants, Saturn F-1, SpaceX Raptor Vacuum, and several others. A Nelder-Mead optimizer is leveraged to search the ten-dimensional radius profile space to maximize thrust for each engine at its design condition. Results show consistent thrust improvements across all configurations, with sea-level optimized engines showing larger percentage gains than vacuum engines. The simulation produces important results that are consistent with compressible flow theory and provides a foundation for more in-depth multicondition optimization work.

1: Introduction

1.1 Motivation

Fuel and combustion chambers are typically the focal points when considering the primary factors contributing to a rocket's power. However, the nozzle is one of the most important yet often overlooked engine components. In a propulsion system, the nozzle converts high-pressure gas from the combustion chamber into thrust. If a nozzle is not designed well, most energy will be lost before the gas can perform work, regardless of the pressure in the combustion chamber.

Nozzle design is challenging because there is no single shape or design that works well everywhere. A rocket travels through continuously changing atmospheric conditions, starting at around 101 kPa at sea level and dropping to almost zero pressure in space. A nozzle optimized for sea level will not perform well at a higher altitude because the exhaust gas will over-expand past the ambient pressure and lose energy to shocks. On the other hand, a nozzle designed for

vacuum will struggle at sea level because the high ambient pressure compresses the exhaust back into the nozzle before it reaches the exit plane. Every fixed nozzle geometry involves a tradeoff, and understanding how that tradeoff plays out across an entire flight is a significant engineering challenge.

Traditional nozzle design approaches often optimize for a single operating condition, acknowledging that performance might not be optimal in varying conditions [1]. This is a reasonable approach when resources are limited, but it means a large portion of the potential design space is never examined. Since computational tools are more accessible than ever, it is possible to study nozzle performance across a broader range of conditions.

This project investigates the design of nozzles specifically for rocket-propelled vehicles, focusing on the optimal design of supersonic flow through a nozzle to achieve maximum thrust efficiency. Results will be simulated in Python to demonstrate the tradeoffs in design variables and confirm the selection of the optimal design. This project addresses how nozzle geometry tradeoffs play out across an entire flight by building a simulation that evaluates nozzle performance under different operating conditions.

The model is based on established compressible flow theory and is tested with real engines using known performance data. An optimization routine is then leveraged to search for the nozzle geometry that maximizes thrust at a given condition. By comparing the optimized results against real engine baselines, the project provides a clear understanding of where current designs stand relative to their theoretical optimum and what changes would improve performance.

1.2 History of Propulsion and Nozzle Development

The history of rocket propulsion goes back to 13th century China, where rockets were used as weapons and for ceremonies [8]. For most of that history, the shape of the nozzle was not a serious engineering consideration. Early rockets utilized directed combustion with little research into how exit geometry affected thrust. The energy was in the propellant, but extracting it efficiently was a problem that would not be meaningfully addressed for several more centuries [8].

The major change in nozzle theory came in the late 19th century when Swedish engineer Gustaf de Laval developed the converging-diverging nozzle while working on steam turbine technology [2]. He demonstrated that by accelerating a flow through a converging section to Mach 1 at the throat and then allowing it to expand through a diverging section, supersonic exit velocities could be achieved [2]. This was not obvious at the time, since most engineers thought that a larger exit area would simply slow the flow down, just as a river slows when it widens. However, supersonic flow works the opposite way, and once the flow reaches Mach 1 at the throat, a wider channel actually speeds it up further [2]. The de Laval nozzle proved otherwise and became the foundation of modern rocket nozzle design.

Through the 20th century, engineers developed rigorous mathematical tools for nozzle design, such as the method of characteristics [3], which allows for the design of contours that minimize shock formation and produce uniform supersonic exit flow. These methods shaped the nozzles of early ballistic missiles including the V-2 and later the Saturn V engines. The introduction of computational fluid dynamics then changed what was possible, allowing engineers to simulate real-gas effects that analytical methods could only approximate, and opening the door to computational optimization as a standard part of the design process.

1.3 Current State of Research

Modern nozzle optimization draws from a wide range of computational methods. Rao [4] showed that genetic algorithms could outperform traditional design methods on nozzle shape optimization problems, helping establish population-based methods as a credible approach for this class of problem.

More recently, surrogate modeling techniques including Gaussian process regression and neural networks have been used to reduce the computational cost of optimization by approximating the relationship between geometry and performance [5]. This allows many more possible designs to be evaluated than would be feasible with full simulations at every step. This project contributes to this area by applying an optimization method directly to the nozzle radius profile. It treats the full contour shape as the design variable rather than limiting the search to a small number of parameters. However, the method used here is considerably simpler in scope than these surrogate-based approaches. Rather than training a model to approximate the objective function, the Nelder-Mead algorithm examines the 1D isentropic flow equations directly at each potential design.

1.4 Project Overview

This project develops a simulation for rocket nozzle design based on one-dimensional isentropic flow theory. The nozzle geometry is defined by a discrete radius profile along the diverging section, and thrust is evaluated for a given set of chamber conditions and ambient pressure. Fourteen real engine configurations are modeled and compared using a normalized performance metric. An optimization routine using the Nelder-Mead method employs to search through the radius profile to find the geometry that maximizes thrust for each engine. Results are presented as comparisons between the baseline and optimized designs, with analysis of what geometric changes the optimizer made and why they improve performance.

2: Background

2.1 Rocket Propulsion Fundamentals

Rocket propulsion is based on Newton's third law. By expelling mass at high velocity from a vehicle's exhaust, a reaction force is generated that propels it forward. The efficiency of this process is measured by specific impulse, defined as thrust per unit weight flow rate of propellant,

$$Isp = \frac{F}{\dot{m} * g_0}$$

Here, F is thrust, $\dot{m}$ is mass flow rate, and g_0 = 9.81 $\frac{m}{s^2}$. Specific impulse has units of seconds and does not depend on engine scale, which makes it a useful figure of merit for comparing engines of different sizes. A higher specific impulse means the engine produces more thrust per unit of propellant consumed, which matters significantly because propellant mass typically dominates the total vehicle mass at liftoff.

The Tsiolkovsky rocket equation shows directly how specific impulse affects mission capability. The achievable change in velocity depends on the specific impulse and the ratio of initial to final vehicle mass,

$$\Delta v = Isp * g_0 * ln(\frac{m_{initial}}{m_{final}})$$

Because the relationship is logarithmic, even modest improvements in specific impulse translate into meaningful increases in payload capacity for a given vehicle size.

2.2 Nozzle Design and the de Laval Geometry

The converging-diverging nozzle accelerates combustion gases from subsonic to supersonic speeds. The flow accelerates through the converging section, reaching Mach 1 at the minimum area throat, and then continues to accelerate supersonically through the diverging section as the area increases.

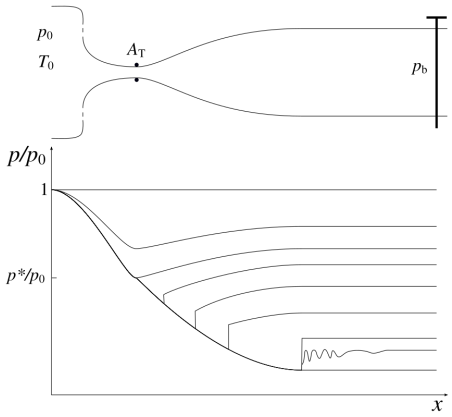

Figure 1: Picture of a converging-diverging nozzle with pressure profiles for different operating conditions [6].

The relationship between local area and Mach number for isentropic flow is

$$\frac{A}{A^*} = \frac{1}{M}\left[\frac{2}{\gamma+1}\left(1 + \frac{\gamma-1}{2}M^2\right)\right]^{\frac{\gamma+1}{2(\gamma-1)}}$$

where A* is the throat area and Gamma is the ratio of specific heats. For any area ratio greater than one, this equation has two solutions, one subsonic and one supersonic. The supersonic root is the relevant one for the diverging section and is solved numerically given a known expansion ratio.

Three operating conditions define how a nozzle performs relative to its environment. A perfectly expanded nozzle has exit pressure equal to ambient pressure, which produces maximum thrust because all available pressure energy has been converted to exhaust velocity. An under-expanded nozzle has exit pressure above ambient, meaning the flow leaves the nozzle with residual pressure that could have been converted to additional velocity with a larger exit area. An over-expanded nozzle has exit pressure below ambient, causing oblique shocks to form and in severe cases, leading to flow separation inside the nozzle, reducing efficiency and potentially causing structural loading on the nozzle walls.

2.3 Thrust Generation

Total thrust from a rocket nozzle comes from two contributions: the momentum of the exhaust gas and the pressure force at the exit plane. For a nozzle in which the diverging section expands at an angle Theta from the centerline, a divergence efficiency factor is applied to account for exhaust momentum that is directed off-axis:

$$F = \eta \dot{m} V_e + (P_e - P_a) A_e$$

where Eta is the divergence efficiency, mass flow rate, Ve is exit velocity, Pe is exit pressure, Pa is ambient pressure, and Ae is exit area. For a conical nozzle with half-angle Theta, the divergence efficiency is:

$$\eta = cos(\theta)$$

This correction accounts for the fact that exhaust exiting at angle Theta from the axis contributes only the axial component of its momentum to the thrust vector. A larger half-angle therefore wastes a greater fraction of the exhaust momentum on radial velocity that does not contribute to thrust.

The presence of the pressure term shows that ambient pressure directly affects thrust performance. At sea level, ambient pressure is approximately 101 kPa, and the pressure thrust contribution depends on how closely the exit pressure matches that value. As the rocket ascends and ambient pressure decreases, a larger expansion ratio becomes more helpful because the lower ambient pressure lets the gas expand further before leaving the nozzle. At sea level, an expansion ratio that is too great drives the exit pressure below ambient and leads to over-expansion with shock losses.

2.4 Isentropic Flow Relations

For an ideal gas expanding isentropically through a nozzle, all exit conditions are determined by the chamber stagnation conditions and the exit Mach number. The pressure and temperature ratios between the exit and the chamber are

$$\frac{P_e}{P_c} = [1 + (\frac{\gamma-1}{2}) M_e^{\,2}]^{\frac{-\gamma}{\gamma-1}}$$

$$\frac{T_e}{T_c} = [1 + (\frac{\gamma-1}{2}) M_e^{\,2}]^{-1}$$

where P_c and T_c are the chamber stagnation pressure and temperature and Me is the exit Mach number. Exit velocity is then computed from the Mach number and the local speed of sound at the exit

$$V_e = M_e * \sqrt{\gamma * R * T_e}$$

where R is the specific gas constant for the combustion products. Mass flow rate is set by the choked throat condition and depends only on chamber conditions and throat area:

$$\dot{m} = A_t * P_c * \sqrt{\frac{\gamma}{R * T_c}} * [\frac{2}{\gamma+1}]^{\frac{\gamma+1}{2(\gamma-1)}}$$

These five equations form the complete analytical model. Given chamber pressure, temperature, specific heat ratio, gas constant, throat area, and expansion ratio, the full thrust solution is determined. The gas constant and specific heat ratio vary between engine configurations to reflect differences in propellant chemistry, which is an important source of performance variation across the engines studied.

Metric	Original	Optimized	Delta
Thrust	336.71 kN	338.01 kN	+0.39%
Isp	287.5 s	288.6 s	+1.1 s
Exit Mach	3.092	3.198	+0.106
Epsilon	7.17	8.28	+1.10
Half-angle	10.6°	11.9°	+1.2°
Exit Pressure	390.3 kPa	321.5 kPa	-68.8 kPa

Table 1: Exit Mach number as a function of expansion ratio from the isentropic area-Mach relation, with original and optimized operating points marked for comparison.

2.5 Nozzle Geometry and Parameterization

In this study, the nozzle diverging section is defined by a discrete radius profile: a vector of N = 10 radius values distributed evenly along the fixed axial length L. The cross-sectional area at each station is:

$$A[i] = \pi r[i]^2$$

The throat area is set by the first profile point and the exit area by the last. The expansion ratio follows as epsilon = $\frac{A_e}{A_t}$. The divergence efficiency is computed from the overall slope between the first and last radius values:

$$\eta = cos(arctan(\frac{r[n-1]-r[0]}{L}))$$

This parameterization gives the optimizer control over both the expansion ratio and the divergence angle through the same set of variables. It is expressive enough to represent a meaningful range of nozzle shapes while keeping each function evaluation fast enough for iterative optimization.

3: Methods and Results

3.1 Assumptions

The flow model in this project is based on one-dimensional isentropic flow theory, which is a standard approach for preliminary rocket nozzle analysis [6]. The working fluid is treated as a calorically perfect gas with constant specific heat ratio gamma and gas constant R. Flow is assumed to be steady, one-dimensional, inviscid, and adiabatic. The throat is assumed to be choked at all operating conditions, so the mass flow rate is determined entirely by chamber conditions and throat area. Heat transfer to the nozzle walls, combustion non-uniformities, and multi-phase flow effects are not included. The only real-world correction applied is the cosine divergence factor on the momentum thrust term, which captures the most significant geometric efficiency loss without requiring a full three-dimensional flow solution.

These assumptions are consistent with the level of fidelity used in comparable preliminary design studies. The model will overpredict absolute thrust values compared to a full CFD simulation since large losses are not included, but the relative comparisons between configurations and the trends across flight conditions are important and capture the behavior of the system.

3.2 Engine Configurations

14 real engine configurations are modeled to validate the simulation and compare performance across different design philosophies. The engines cover a range of chamber pressures, propellant types, and operating environments, from small commercial engines like the Rutherford to high-performance staged combustion designs like the RD-180 and Raptor Vacuum. Chamber pressure, temperature, specific heat ratio, and gas constant for each engine are set to approximate published values from available technical documentation.

A normalized optimality score is computed for each engine that accounts for both the magnitude of thrust and how well the exit pressure is matched to the ambient condition. Designs that operate far from their ideal expansion point are penalized, and all scores are normalized to the highest-performing engine so results fall on a zero to one scale.

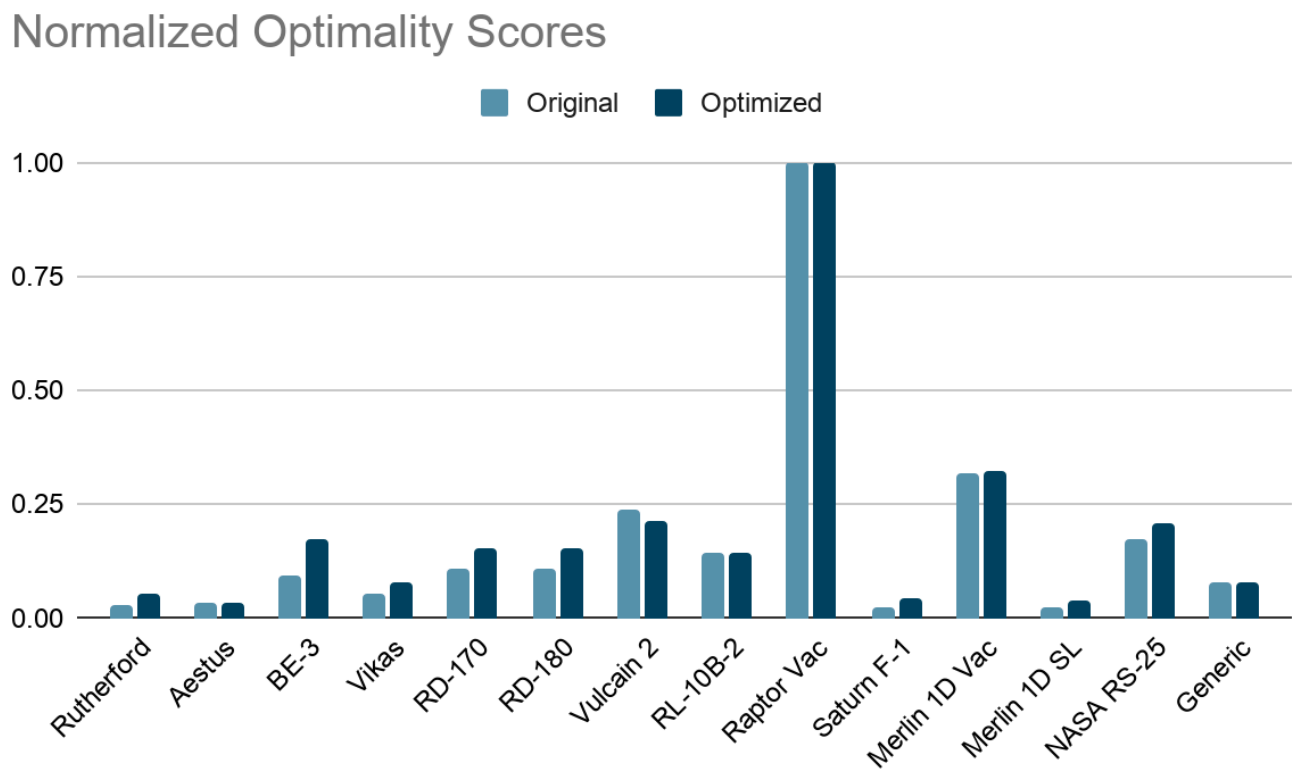

Table 2: Optimality scores for all engine configurations, showing original and optimized performance on a 0 to 1 scale.

3.3 Simulation Procedure

For each engine configuration, the nozzle is initialized with a linear radius profile between the throat radius and a specified exit radius. The exit Mach number is computed by numerically solving the area-Mach [4] relation using a root-finding algorithm with a supersonic initial guess, ensuring the supersonic solution branch is returned. Exit pressure, temperature, and velocity are then computed from the isentropic relations. Mass flow rate is calculated from the choked throat condition. Thrust is assembled from the momentum and pressure terms with the divergence correction applied.

The same procedure is used for every function evaluation during optimization, which keeps the cost of each evaluation low and ensures rapid iteration in the optimizer. The model is implemented in Python using NumPy for array operations and SciPy for the root-finding and optimization routines. All engine configurations are solved and compared before optimization is run, providing a performance baseline and confirming the model produces physically reasonable results.

3.4 Optimization Setup

The optimization is run on each engine configuration using the Nelder-Mead method, a derivative-free simplex algorithm suited to problems where the objective function is not analytically differentiable [7]. The algorithm maintains a simplex of N+1 candidate points in the design space and iteratively updates it through reflection, expansion, contraction, and shrink operations based on objective function values at each vertex [7]. No gradient information is required, which makes it practical here since the relationship between the radius profile and thrust is evaluated numerically.

The design variable is the full radius profile vector of N = 10 values. Three constraints are enforced through penalty returns. The first profile point must remain fixed at the throat radius to keep throat area constant across all evaluated designs. All radius values must fall within bounds between the throat radius and fifty times the throat radius, corresponding to a maximum expansion ratio of approximately 2500. Designs that violate any of these constraints return a large penalty value instead of a thrust calculation, effectively excluding them from the search.

The objective function is the negative of thrust since Nelder-Mead minimizes by default. The optimizer runs for a maximum of 800 iterations starting from the initial linear profile, and returns the radius profile that produced the lowest objective value, corresponding to the highest thrust found during the search.

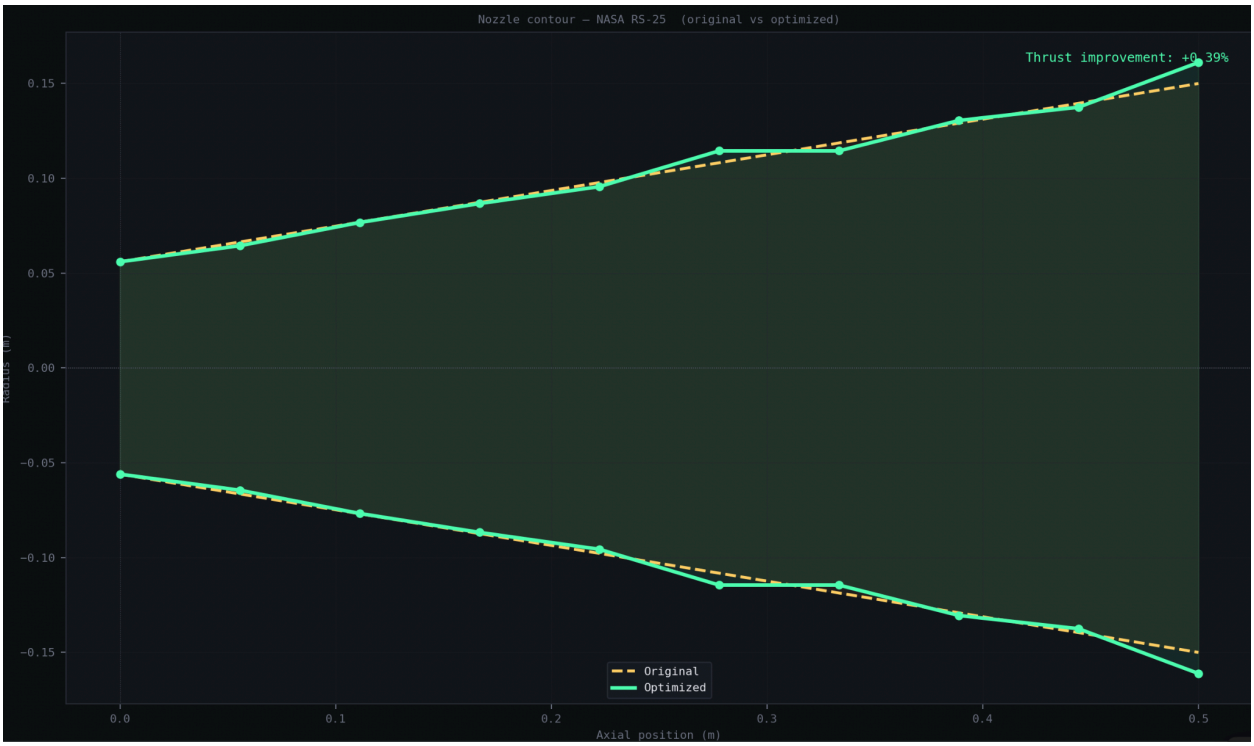

Figure 2: Original vs. optimized nozzle radius profile along the axial direction, showing how the optimizer modified the contour shape relative to the initial linear profile.

3.5 Results

The optimization produced measurable improvements in thrust across all engine configurations. The optimized radius profiles are different from the initial linear profiles in the shape of the intermediate contour, with the optimizer finding expansion paths that better match exit pressure to the ambient condition each engine was designed for, either sea level at 101,325 pascals or vacuum at 0 pascals. Both exit Mach number and total thrust increased relative to the baseline in every case, with the improvement attributed primarily to the optimizer adjusting the effective expansion ratio and divergence angle simultaneously rather than treating them as independent variables.

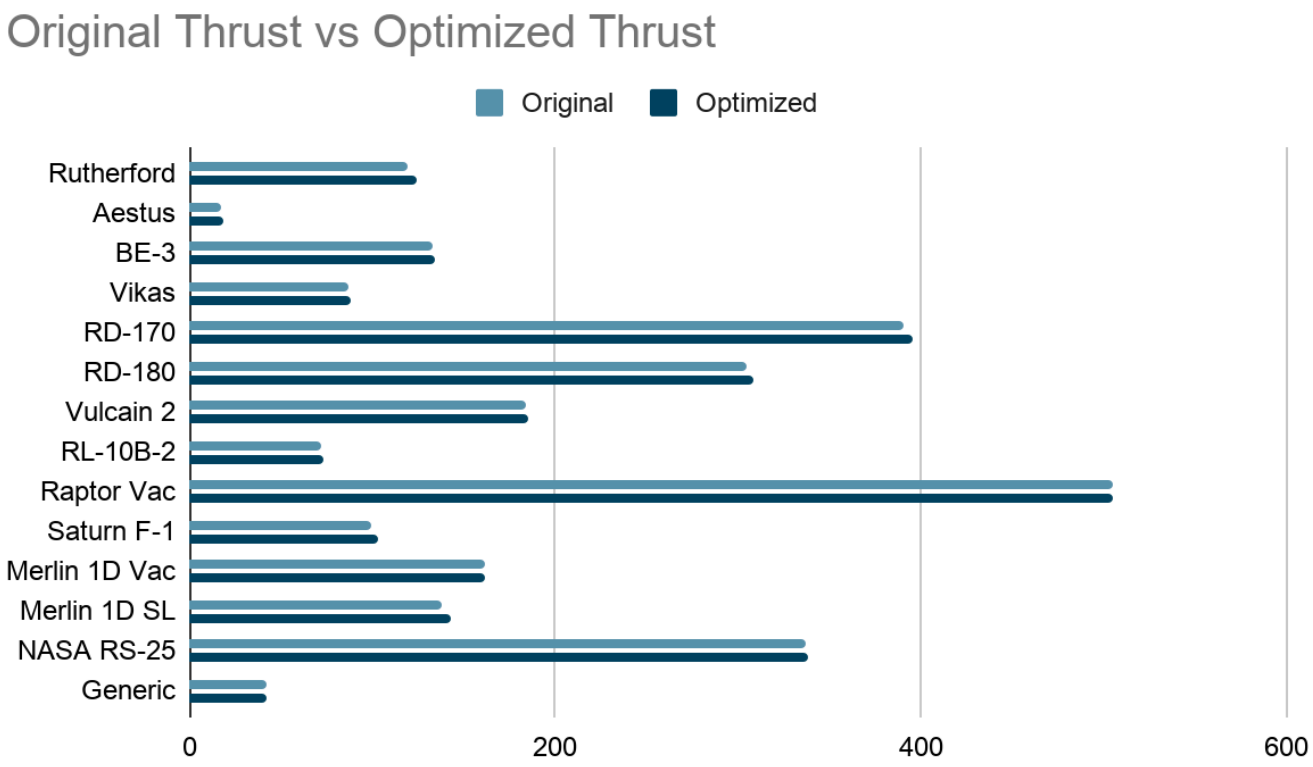

Table 3: Thrust comparison between original and optimized configurations across all engine types, showing percentage improvements for each.

Across the 14 engine configurations, the normalized optimality scores reflect the expected behavior from compressible flow theory. Vacuum-optimized engines score higher when evaluated at low ambient pressure because their large expansion ratios produce exit pressures well matched to the near-vacuum environment. Sea-level engines perform well at their design condition but degrade at altitude as ambient pressure drops and their expansion ratio becomes insufficient. The Merlin 1D sea-level and vacuum variants illustrate this trade-off clearly, since both share similar chamber conditions but are designed for fundamentally different operating environments.

The pressure thrust term dominates performance at high altitude. This explains why vacuum engines benefit from larger expansion ratios, even when the associated increase in divergence angle slightly reduces momentum thrust efficiency. At sea level, a smaller expansion ratio avoids over-expansion and the shock losses that come with it. The model consistently captures this behavior across all configurations, and the optimization results reinforce it by finding geometries that balance exit pressure matching against divergence efficiency in a way that the initial linear profiles do not.

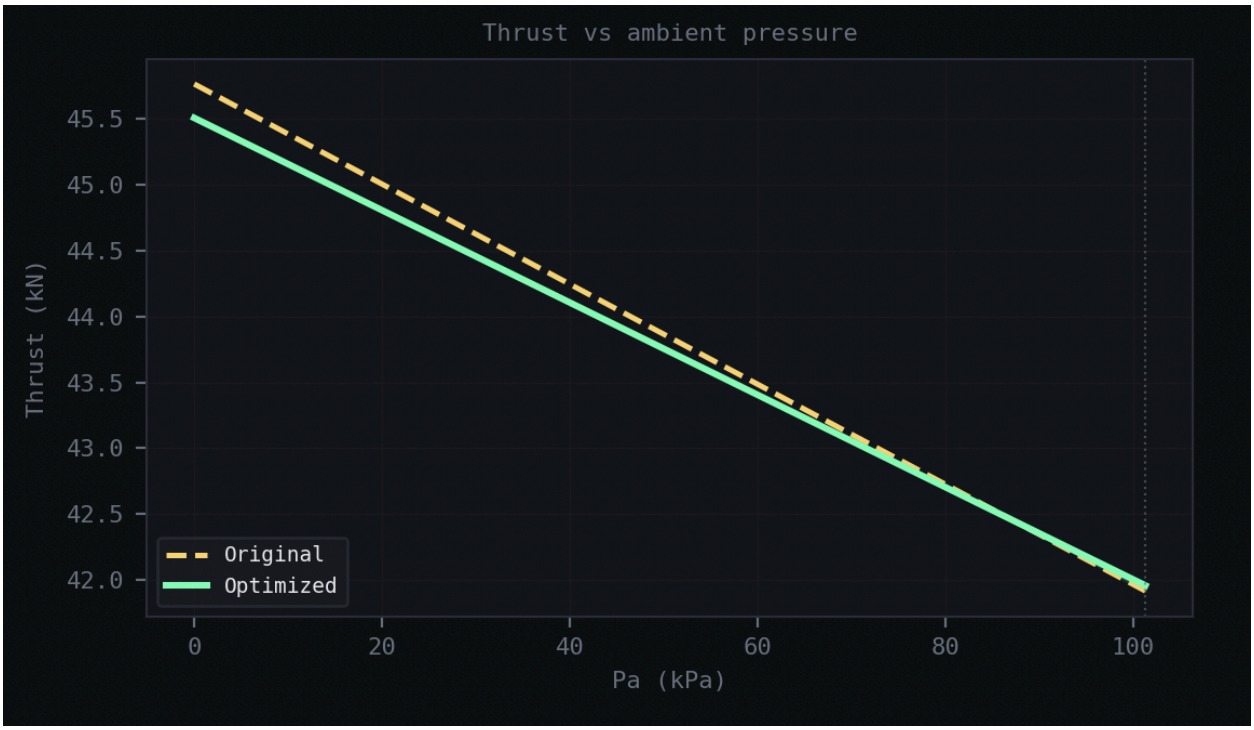

Figure 3: Thrust vs. ambient pressure for the baseline and optimized nozzle, showing performance across the ascent profile from sea level to vacuum and where each design is most effective.

These results confirm that the simulation behaves consistently with established theory and that the optimization is finding real improvements rather than numerical artifacts. The percentage gains, ranging from around 0.01% to 0.05% across the 14 configurations, are small because the Nelder-Mead method is limited to optimizing the radius profile shape given a fixed throat area and chamber conditions. This limitation means the optimizer can only adjust how the flow expands rather than the fundamental energy available. Additionally, the initial linear profiles already represent a reasonable baseline, leaving limited room for improvement within the same design constraints.

Conclusion

This project set out to answer whether, given that no fixed nozzle geometry is optimal at every altitude, performance improves meaningfully when the shape is determined by an optimizer rather than an analytical template. Based on the results across 14 engine configurations, the gains are real and consistent, but they are not large.

The simulation successfully captures the relevant physics of isentropic nozzle flow, reproducing expected performance characteristics across all the engine configurations at their respective design conditions. By allowing the optimizer to simultaneously adjust expansion ratio and divergence angle rather than treating them independently, the model identifies contour modifications that produce consistent thrust improvements across every configuration tested. The fact that these improvements are larger for sea-level engines than for vacuum engines is physically meaningful rather than coincidental. Vacuum engines are already designed with large expansion ratios to take advantage of the absence of ambient back-pressure, placing them closer to their theoretical optimum from the outset. Sea-level engines, by contrast, operate under a tighter pressure-matching constraint, leaving more room for the optimizer to find beneficial adjustments to the exit pressure balance. This pattern of results indicates that the model is responding to the correct underlying physics rather than producing arbitrary numerical outcomes, and that the optimization framework is sensitive to the operating environment in a way that is consistent with established nozzle theory.

The simulation has a few limitations worth acknowledging. The one-dimensional isentropic model overpredicts thrust because it leaves out viscous losses, heat transfer, and boundary layer effects, all of which matter in a real engine. The ten-point radius profile is also a fairly coarse way to represent the nozzle contour, and giving the optimizer more points to work with would open up a wider range of possible shapes. Nelder-Mead is also not guaranteed to find a global optimum, and a population-based method like a genetic algorithm would likely do a better job of exploring the full design space. Improving on these three areas, higher fidelity flow modeling, a denser contour parameterization, and a more robust optimizer, would be the logical next steps toward results that more closely reflect what a real engineering analysis would produce.

A more interesting direction for future work is multi-condition optimization. A nozzle optimized for sea-level thrust is not necessarily the one that gives the best performance over an entire flight, since ambient pressure drops continuously with altitude and the optimal expansion ratio shifts accordingly. Solving for a geometry that performs well across the full flight envelope rather than at a single design point is a harder problem, but a more practically useful one. The simulation developed here is a natural stepping stone toward that goal, since extending it to multi-condition optimization would primarily involve reformulating the objective function to integrate thrust over an altitude profile rather than evaluating it at a single ambient pressure.

Ultimately, this project reinforces that nozzles are not a passive exit for combustion products but an active design element with significant leverage over system performance, and treating its geometry as an optimizable variable rather than a fixed parameter opens up a design space that classical methods do not explore.

Bibliography

[1] “Nozzle Design | Glenn Research Center | NASA,” *Glenn Research Center | NASA*, Nov. 20, 2023. https://www1.grc.nasa.gov/beginners-guide-to-aeronautics/nozzle-design/ (accessed May 24, 2026).

[2] G. V. R. Rao, “Exhaust Nozzle Contour for Optimum Thrust | Journal of Jet Propulsion,” *Journal of Jet Propulsion*, 2025, https://doi.org/10.2514/jjp.1958.28.issue-6;website:website:aiaa-site;wgroup:string:AIAA.

[3] R. Shyne, T. Keith, Orlando, and Florida, “Analysis and Design of Optimized Truncated Scarfed Nozzles Subject to External Flow Effects,” 1990. Accessed: May 24, 2026. [Online]. Available: https://ntrs.nasa.gov/api/citations/19900015790/downloads/19900015790.pdf

[4] J. Mattingly, W. Heiser, D. Pratt, and J. Przemieniecki, “Aircraft Engine Design Second Edition dA-~A4- EDUCATION SERIES,” May 2026. Accessed: May 24, 2026. [Online]. Available: https://dpl6hyzg28thp.cloudfront.net/media/Aircraft_Engine_Design_Second_Edition_Jack_D_6BsGax1._Mattingly.pdf

[5] shurik.kuzmin4586, “The Computer Journal 1965 Nelder 308 13,” *Scribd*, 2026. https://www.scribd.com/document/359617442/The-Computer-Journal-1965-Nelder-308-13 (accessed May 24, 2026).

[6] O. Cleyen, *Wikimedia Commons*, Feb. 2015. https://commons.wikimedia.org/wiki/File:Converging-diverging_nozzle,_pressure_distribution_during_acceleration_of_flow.svg (accessed May 24, 2026).

[7] votatera, “De Laval Nozzle | Thrust Efficiency & Speed Control,” *Modern Physics Insights: Discover, Understand, Innovate*, May 26, 2024. https://modern-physics.org/de-laval-nozzle/ (accessed May 24, 2026).

[8] “A Brief History Of Rockets,” *web.eng.fiu.edu*. https://web.eng.fiu.edu/allstar/rocket-history.htm (accessed May 24, 2026).

[9] “ENHANCED DATA EFFICIENCY USING DEEP NEURAL NETWORKS AND GAUSSIAN PROCESSES FOR AERODYNAMIC DESIGN OPTIMIZATION,” *arXiv.org*, Aug. 18, 2020. https://arxiv.org/pdf/2008.06731 (accessed May 24, 2026).